Journal of Medicinal Chemistry

Brief Article

pubs.acs.org/jmc

Structure-Based Optimization of a Peptidyl Inhibitor against Calcineurin-Nuclear Factor of Activated T Cell (NFAT) Interaction

Ziqing Qian,[†] Patrick G. Dougherty,[†] Tao Liu,[†,§] Shameema Oottikkal,[†] Patrick G. Hogan,[‡] Christopher M. Hadad,[†] and Dehua Pei*[,†]

[†]Department of Chemistry and Biochemistry, The Ohio State University, 484 West 12th Avenue, Columbus, Ohio 43210, United States

[‡]Division of Signaling and Gene Expression, La Jolla Institute for Allergy and Immunology, La Jolla, California 92037, United States

Supporting Information

ABSTRACT: Calcineurin inhibitors such as cyclosporine A and FK506 are effective immunosuppressants but produce severe side effects. Rational modification of a previously reported peptide inhibitor, GPHPVIVITGPHEE (K_D ~ 500 nM), by replacing the two valine residues with *tert*-leucine and the C-terminal proline with a *cis*-proline analogue, gave an improved inhibitor ZIZIT-*cis*Pro, which binds to calcineurin with a K_D value of 2.6 nM and is more resistant to proteolysis.

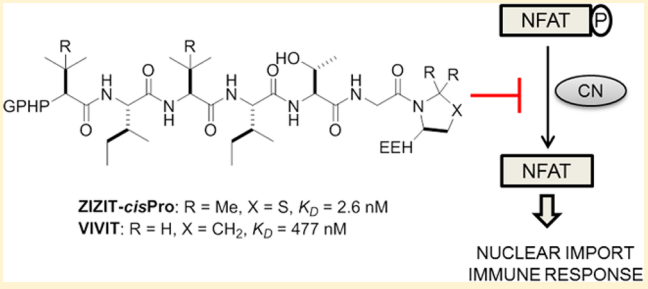

INTRODUCTION

Calcineurin (CN) is a protein serine/threonine phosphatase involved in T cell signaling. Engagement of T cell-surface receptors with ligands (e.g., an antigen-presenting cell) causes an increase in the cytoplasmic level of calcium, which activates many calmodulin (CaM)-dependent enzymes including CN. CN dephosphorylates multiple phosphoserines on nuclear factor of activated T cell (NFAT), a transcription factor, leading to its nuclear translocation and activation.[1,2] The activated NFAT up-regulates the expression of interleukin 2 (IL-2), which in turn activates T-helper lymphocytes, induces the production of other cytokines, and stimulates the immune response. CN is the target of several naturally occurring macrocycles such as cyclosporine A (CsA) and FK506. These compounds bind to cellular proteins cyclophilin and FKBP12, respectively, and the resulting binary complexes bind to CN and sterically block the access of NFAT and other protein substrates to the CN active site.[3] CsA and FK506 are clinically used as immunosuppressants in postallogenic organ transplant.[4] Nevertheless, treatment with these drugs is associated with severe side effects including nephrotoxicity and hepatotoxicity,[5] likely because of their indiscriminate inhibition of CN activity toward all substrates.[6−8] Inhibitors that selectively block the CN−NFAT interaction would provide less toxic immunosuppressants.

Previous structural and functional analysis of the CN−NFAT interface has identified a conserved sequence motif among NFAT proteins, PxIxIT (where x is any amino acid), which specifically interacts with a substrate-docking site on CN.[9] This interaction is critical for dephosphorylation of NFAT and a subset of other CN substrates.[10−12] Screening of an oriented peptide library identified a tetradecapeptide, GPHPVIVITGPHEE (VIVIT, Table 1), which binds to the docking site on CN with 25-fold higher affinity than the naturally occurring PxIxIT motif.[13] Expression of peptide VIVIT in mammalian cells effectively blocks the CN−NFAT interaction and its downstream signaling without directly blocking CN enzymatic activity. Attachment to a cell-penetrating peptide (R_{11}) renders the peptide cell permeable and active for immunosuppression in transplanted mice.[14] This observation has inspired investigators to develop peptides and small molecules as selective CN inhibitors.[15] However, the reported compounds have somewhat low potency in disrupting the CN−NFAT interaction. In this work, we used the structural information derived from previous NMR and X-ray studies[16−18] as a guide and carried out a structure-based optimization of the VIVIT peptide, which led to ~200-fold improvement in the binding affinity and a highly potent and selective inhibitor against CN (K_D = 2.6 nM).

Table 1. Sequences and Dissociation Constants of Peptidyl Ligands

peptide	sequence[a]	K_D (nM)[b]
VIVIT	GPHPVIVITGPHEE	477 ± 26
ZIZIT	GPHPZIZITGPHEE	43 ± 12
ZIZIT-*cis*Pro	GPHPZIZITGP*HEE	2.6 ± 0.8
VAVAA	GPHAVAVAAGPHEE	>200000

[a]Z, *tert*-leucine; P*, Cys($\Psi^{Me,Me}$Pro). [b]K_D values against CN were obtained from FA assay using N-terminal 5(6)-SFX labeled peptides.

Received: May 13, 2014
Published: August 27, 2014

   dx.doi.org/10.1021/jm500743t | J. Med. Chem. 2014, 57, 7792−7797

RESULTS AND DISCUSSION

Substitution of *tert*-Leucine (Tle) for Valine. The structure of the CN–VIVIT complex[16,17] reveals that the PVIVIT core is in an extended conformation and engages in hydrophobic, van der Waals, and hydrogen bonding interactions with CN. The side chains of three highly conserved residues, Pro[4], Ile[6], and Ile[8], fit snugly into three well-defined hydrophobic pockets, while the side chains of Val[5] and Val[7] are largely solvent exposed (Figure 1A). The PVIVIT core also forms multiple hydrogen bonds between its backbone amides and CN β-strand 14 residues.[16,18] We suspected that substitution of Tle for Val[5] and Val[7] of the peptide ligand might improve its potency and/or bioavailability, based on several considerations. First, the Val[5] and Val[7] side chains are distant from the hydrophobic surface formed by the side chain of CN Val[328] for optimal van der Waals interaction. Replacement of the valines with bulkier Tle should result in closer packing between Tle[5]/Tle[7] and Val[328] side chains and improved van der Waals interactions between them. Second, Tle is frequently used as building blocks for peptidomimetic drugs[19,20] and organocatalysts[21] because incorporation of Tle has been shown to substantially improve the target-binding affinity, protease resistance, and/or bioavailability.[22,23] While the increased stability against proteolysis (and nonenzymatic hydrolysis of the peptide bond) can be attributed to the steric hindrance exerted by the *t*-butyl side chain, the origin of the increased binding affinity and membrane permeability is less clear. It has been speculated that the bulky *t*-butyl group may interfere with solvation of the adjacent peptide bonds and therefore decrease the amount of desolvation energy associated with target binding and membrane transport. We therefore replaced both Val[5] and Val[7] with Tle and named the resulting peptide "ZIZIT" (where Z = Tle). Peptide ZIZIT was synthesized using standard solid-phase peptide chemistry and 2-(7-aza-1*H*-benzotriazole-1-yl)-1,1,3,3-tetramethyluronium hexafluorophosphate (HATU) as the coupling reagent. To our delight, peptide ZIZIT bound to CN with a 10-fold higher affinity than VIVIT (K_D values of 43 ± 12 and 477 ± 26 nM, respectively) (Table 1 and Figure 2A).

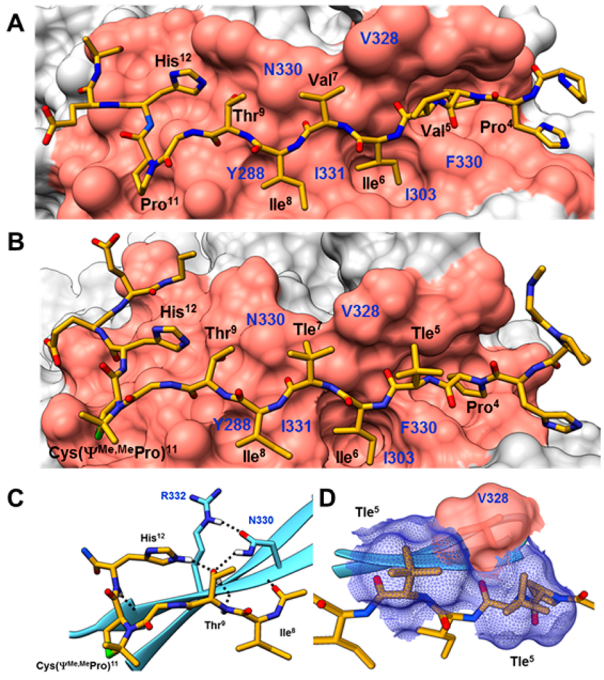

Figure 1. (A) X-ray crystal structure of the CN–VIVIT complex (the image was generated from pdb file 2P6B[13] with Chimera[28]). (B) Binding mode of peptide ZIZIT-*cis*Pro to CN as derived from MD simulations. CN is displayed as the van der Waals surface with the binding surface shaded solid pink and the rest colored gray. Peptide ligands are shown as sticks with carbon, nitrogen, oxygen, and sulfur atoms in yellow, blue, red, and green, respectively. Key ligand residues are labeled in black three-letter codes, while CN residues are labeled in blue single-letter codes. Tle, *tert*-leucine. (C) A close-up view of the hydrogen-bond network between CN (in cyan) and ligand residues adjacent to the *cis*-proline analogue (in yellow). (D) van der Waals surface contours of Val[328] of CN and Tle[5] and Tle[7] of the peptide ligand.

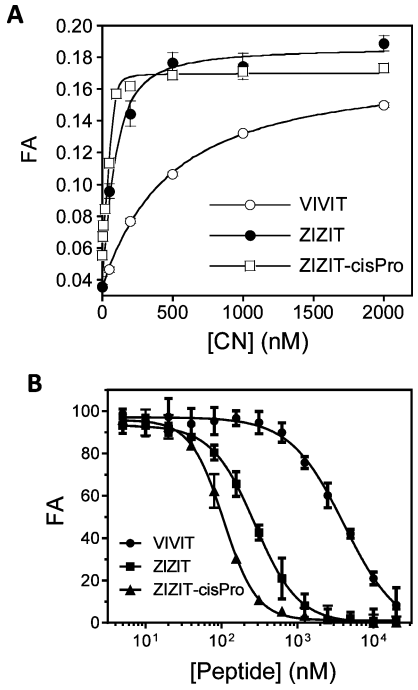

Figure 2. Comparison of the binding affinities of peptides VIVIT, ZIZIT, and ZIZIT-*cis*Pro to CN. (A) Plot of fluorescence anisotropy of FITC-labeled peptides (100 nM) as a function of CN concentration. (B) Plot of FA of FITC-labeled ZIZIT (100 nM) in the presence of CN (150 nM) and unlabeled peptides VIVIT, ZIZIT, or ZIZIT-*cis*Pro (0–20 μM) as a function of the competing peptide concentration. Data reported were the mean ± SD from three independent experiments. The FA values in (B) were relative to that in the absence of competing peptide.

Incorporation of Cys($\Psi^{Me,Me}$Pro) as *cis*-Pro Analogue. The structure of the CN–VIVIT complex[16,17] contained a *cis* peptide bond between Gly[10] and Pro[11] of VIVIT (Figure 1A). The β-turn structure permits the formation of an intricate hydrogen bond network among the side chains of Asn[330] (of CN) and His[12] and Thr[8] of the VIVIT peptide.[16] Because the *trans*-configuration of a peptidyl–prolyl peptide bond is energetically more stable,[24] we envisioned that preorganization of the Gly[10]–Pro[11] peptide bond into the *cis*-configuration should increase the binding affinity. 2,2-Dimethylthiazolidine [Cys($\Psi^{Me,Me}$Pro)] has previously been used as a proline analogue; when it is incorporated into a peptide, the preceding peptide bond is sterically locked into the *cis*-configuration.[25,26]

dx.doi.org/10.1021/jm500743t | J. Med. Chem. 2014, 57, 7792–7797

We thus designed peptide ZIZIT-*cis*Pro (Figure 1B) by replacing Pro[11] of ZIZIT with Cys($\Psi^{Me,Me}$Pro).

Synthesis of peptide ZIZIT-*cis*Pro is illustrated in Figure S1 in Supporting Information (SI). Briefly, the sterically hindered secondary amine of 2,2-dimethyl-1,3-thiazolidine-4-carboxylic acid [H-Cys($\Psi^{Me,Me}$Pro)-OH] is poorly reactive and cannot be directly incorporated into peptides through solid-phase synthesis. Thus, the pseudoproline was first prepared as the Fmoc-protected dipeptide, which was readily introduced into peptides using benzotriazol-1-yl-oxytripyrrolidinophosphonium hexafluorophosphate (PyBop) as the coupling reagent.[27] The dipeptide, Fmoc-Gly-Cys($\Psi^{Me,Me}$Pro)-OH, was prepared in 69% yield by condensing Fmoc-protected glycyl fluoride and H-Cys($\Psi^{Me,Me}$Pro)-OH.[27] Because Cys($\Psi^{Me,Me}$Pro) is unstable under strongly acidic conditions (e.g., 100% TFA), acid-labile side chain protecting groups 4-methyltrityl (Mmt), 2-phenylisopropyl (Ph*i*Pr), and trityl (Trt) were employed for His, Glu, and Thr residues, respectively. After the fully protected peptide was synthesized on solid phase, these side chain protecting groups were removed by treatment under a mildly acidic condition (1% TFA, 5% triisopropylsilane in DCM, 2 h), which did not significantly damage the Cys($\Psi^{Me,Me}$Pro) moiety. The deprotected peptide was released from the solid support by aminolysis with 1:1 (v/v) propylamine/DMF and purified to near homogeneity by reversed-phase HPLC (Figure S2 in SI).

The binding affinity of ZIZIT-*cis*Pro for CN was determined by fluorescence anisotropy (FA). Incorporation of the *cis*-proline analogue further increased the binding affinity of ZIZIT for CN by ~20-fold, producing a highly potent peptidyl inhibitor against CN (K_D = 2.6 nM, Figure 2A). The change in affinity is consistent with increasing the *cis* peptidyl−prolyl bond population from its normal abundance (5−10%) to ~100% in ZIZIT-*cis*Pro.[25−27]

Binding Site, Selectivity, and Serum Stability of ZIZIT-*cis*Pro. To determine whether ZIZIT and ZIZIT-*cis*Pro bind to the same site as VIVIT on CN, we modified the FA assay to test the competition among the three peptides for binding to CN. Briefly, peptide ZIZIT, which has an intermediate binding affinity (K_D = 43 nM), was labeled with fluorescein isothiocyanate (FITC) and tested for binding to CN in the presence of increasing concentrations of unlabeled VIVIT, ZIZIT, or ZIZIT-*cis*Pro. All three peptides inhibited the binding of FITC−ZIZIT to CN in concentration-dependent manners, with IC_{50} values of 4100 ± 100, 280 ± 90, and 110 ± 90 nM, respectively (Figure 2B). These data suggest that all three peptides bind to the same site (or overlapping sites) on CN. Further, the ability of ZIZIT-*cis*Pro to largely eliminate FITC−ZIZIT binding at stoichiometric amounts (~150 nM, which was also the CN concentration used) suggests that ZIZIT-*cis*Pro binds to a single site on CN.

To determine whether ZIZIT-*cis*Pro is a specific ligand of CN, we tested it for binding to five arbitrarily selected proteins by FA, including bovine serum albumin (BSA), protein−tyrosine phosphatases 1B (PTP1B), and SHP1, K-Ras G12V, and the SH2 domain of Grb2. ZIZIT-*cis*Pro bound weakly to PTP1B (K_D ~9 μM) and SHP1 (K_D >15 μM) but not to the other three proteins up to 15 μM protein concentration (Figure S3 in SI), indicating that it is a selective ligand of CN.

The proteolytic stability of peptides VIVIT and ZIZIT-*cis*Pro was assessed by incubating the peptides in diluted human serum (25%) at 37 °C and monitoring the amounts of remaining peptides by HPLC. The VIVIT peptide was degraded with a half-life of ~1 h and to completion in 6 h (Figure 3). In contrast, ~60% of ZIZIT-*cis*Pro remained intact after 6 h of incubation. Thus, incorporation of the Tle and/or cis-Pro residues substantially improved the proteolytic stability of the CN ligand.

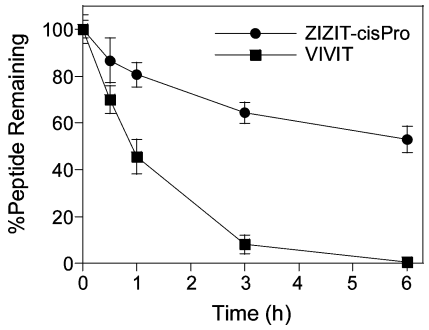

Figure 3. Comparison of the serum stability of peptides VIVIT and ZIZIT-*cis*Pro at 37 °C.

Molecular Modeling. To gain some mechanistic insight into the observed affinity enhancement, we carried out molecular dynamic (MD) simulations on the CN−ZIZIT-*cis*Pro complex. To provide some information about how the new ligand would interact with the CN surface, we proceeded with a molecular docking study; we began by using the available crystal structure of the CN−VIVIT complex (pdb ID 2p6b)[16] and replacing the ligand with ZIZIT-*cis*Pro. Following the construction of ZIZIT-*cis*Pro ligand and energy minimization as detailed in the Experimental Section, MD simulations were performed to obtain the docked conformation.[28] Analysis of the root-mean-square deviation (RMSD) between the crystal structure and MD protein showed no deviation indicative of sudden, chaotic structural fluctuations (Figure S4 in SI). Further, ZIZIT-*cis*Pro remained associated with the binding site on the CN surface throughout the simulation, as indicated by the number of hydrogen bonds between the ligand and the protein (Figure S5 in SI).

ZIZIT-*cis*Pro adopts a virtually identical conformation to that of VIVIT in the crystal structure (Figure 1A,B). The side chains of Ile[6] and Ile[8] are clearly accommodated in hydrophobic pockets formed by Met[329]/Met[290]/Ile[303] and Tyr[288]/Met[290]/Ile[331], respectively. ZIZIT-*cis*Pro engages in the same set of hydrogen bonds with CN as VIVIT. The Gly[10]-Cys-($\Psi^{Me,Me}$Pro)[11] peptide bond is indeed in its *cis*-configuration, thus permitting the formation of the hydrogen bond network between ligand side chains of His[12] and Thr[9] and CN residues Arg[332] and Asn[330] (Figure 1C). The geminal dimethyl groups of the proline analogue are oriented away from the protein surface and do not appear to experience any steric clashes with any protein residue. In contrast to the CN−VIVIT structure, in which Val[5] and Val[7] side chains are solvent exposed,[16] the additional side chain methyl groups in the CN−ZIZIT-*cis*Pro complex result in close packing of the Tle[5] and Tle[7] side chains against the side chain of Val[328] (Figure 1D). In fact, the Tle side chains are ~1 Å closer to the Val[328] side chain than those of Val[5] and Val[7]. These results suggest that enhanced van der Waals interactions and/or hydrophobic effects between the Tle side chains and Val[328] contribute significantly to the observed high potency of the ZIZIT-*cis*Pro ligand. We also calculated the solvent accessible surface area (SASA) of both VIVIT and ZIZIT-*cis*Pro peptides when they are bound to the CN protein using the trajectories derived from the 20 ns MD simulations.

dx.doi.org/10.1021/jm500743t | J. Med. Chem. 2014, 57, 7792−7797

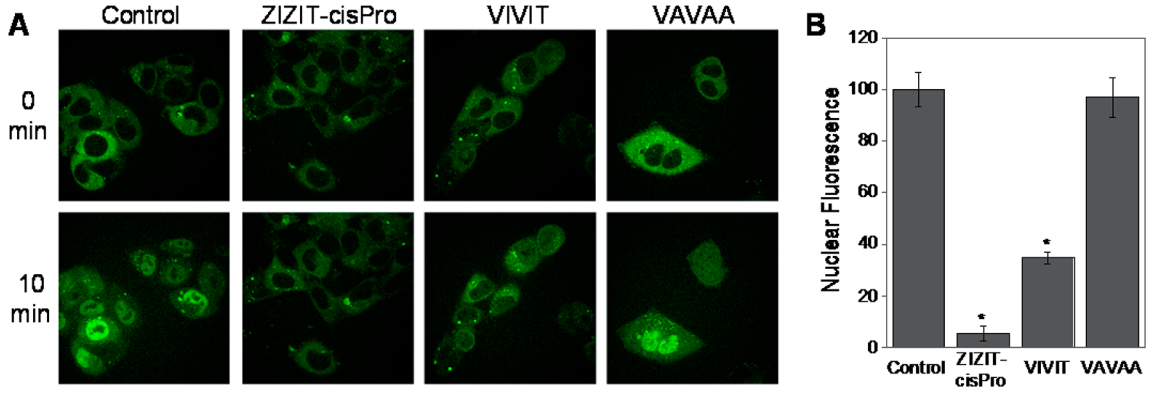

Figure 4. (A) Time-lapse live cell confocal microscopic imaging of HeLa cells stably transfected with GFP−NFAT after stimulation with ionomycin and in the absence or presence of different CN inhibitors (500 nM). (B) Relative potencies of the CN inhibitors in blocking the nuclear translocation of GFP−NFAT. The increase in fluorescence intensity in the nuclear region after 10 min of stimulation with ionomycin was measured and compared to that of control cells (untreated with CN inhibitor; 100%). *, $P < 0.001$ compared with control; two tailed t test. Data reported represent the mean ± SD from at least 30 cells. All CN inhibitors contained R_{11} on their N-termini (Figure S6 in SI).

The calculated SASA values for VIVIT (2123 ± 29 Å^2) and ZIZIT-*cis*Pro (1970 ± 30 Å^2) indicate that ZIZIT-*cis*Pro peptide is less solvated than VIVIT peptide in CN-bound states, providing further support that ZIZIT-*cis*Pro engages in greater van der Waals and/or hydrophobic interactions with the CN protein than the parent peptide.

Inhibition of Nuclear Translocation of NFAT. To test whether the increased binding affinity of ZIZIT-*cis*Pro translates into improved efficacy in cellular assays, we conjugated it to a polybasic cell-penetrating peptide, R_{11}. First, peptide ZIZIT-*cis*Pro was modified at its N-terminus with a bifunctional linker succinimidyl 3-(2-pyridyldithio)propionate (SPDP) (Figure S6 in SI). The resulting peptide was conjugated to R_{11}, which was synthesized with a C-terminal cysteine, via a disulfide exchange reaction. We also prepared R_{11}−VIVIT and a negative control peptide, R_{11}−VAVAA, which contains replacement of three key CN-binding residues (Ile^6, Ile^8, and Thr^9) with alanine and has no detectable binding to CN as judged by FA analysis (Table 1). HeLa cells stably transfected with a green fluorescent protein−NFAT1 fusion (GFP−NFAT)[29] were treated with the peptides in the absence and presence of ionomycin and the intracellular distribution of green fluorescence was monitored by live-cell confocal microscopy (Figure 4A).[14] In control cells (untreated with either ionomycin or peptide), GFP−NFAT was localized predominantly in the cytosol with minimal signal in the nuclear region. Treatment of cells for 10 min with ionomycin, which raises the intracellular Ca^{2+} concentration and activates CN activity, caused translocation of GFP−NFAT into the nucleus, as observed by time-lapse live-cell confocal microscopic imaging. However, incubation of cells with 500 nM R_{11}−ZIZIT-*cis*Pro prior to the treatment with ionomycin almost completely blocked the nuclear translocation of GFP-NFAT (~95% inhibition) (Figure 4B). This potency of peptide R_{11}−ZIZIT-*cis*Pro is similar to that of FK506 in the translocation assay.[14] Under the same conditions, R_{11}−VIVIT resulted in ~65% inhibition of the nuclear translocation. As expected, peptide R_{11}−VAVAA had no detectable effect on the ionomycin-stimulated GFP-NFAT translocation.

■ CONCLUSION

Through relatively minor structural modifications, we were able to improve the CN-binding affinity of peptide VIVIT by ~200-fold. With a K_D value of 2.6 nM, ZIZIT-*cis*Pro ranks among some of the most potent CN inhibitors reported to date.[15] The steric bulk of Tle and/or the *cis*-Pro analogue also improve the proteolytic stability of the peptide. Peptide R_{11}−ZIZIT-*cis*Pro may be further developed into an efficacious but less toxic alternative to FK506 and CsA.

■ EXPERIMENTAL SECTION

Materials. Reagents for peptide synthesis were purchased from NovaBiochem (La Jolla, CA), Peptides International (Louisville, KY), or Chem-Impex International Inc. (Wood Dale, IL). SPDP was obtained from Thermo Scientific (Rockford, IL). 5(6)-Fluorescein-6(5)-carboxamidohexanoic acid, succinimidyl ester [5(6)-SFX, F-6129] was from Life Technologies (Carlsbad, CA).

Peptide Synthesis and Labeling. Peptides were synthesized on Rink Resin LS (0.2 mmol/g) using standard Fmoc chemistry. The typical coupling reaction contained 5 equiv of Fmoc-amino acid, 5 equiv of HATU, and 10 equiv of diisopropylethylamine (DIPEA) and was allowed to proceed with mixing for 1 h. The peptides were deprotected and released from the resin by treatment with 92.5:2.5:2.5:2.5 (v/v) TFA/phenol/water/triisopropylsilane for 2 h. The peptides were triturated with cold ethyl ether and purified by reversed-phase HPLC equipped with a C_{18} column. The peptide (~1 mg in 300 μL of 1:1 (v/v) DMF/150 mM sodium bicarbonate, pH 8.5) was treated with 10 μL of 100 mg/mL 5(6)-SFX in DMSO for 1 h and purified again by HPLC.

Dipeptide Fmoc-Gly-Cys($\Psi^{Me,Me}$Pro)-OH was prepared by mixing Fmoc-Gly-F (420 mg, 1.4 mmol)[30] with 1 equiv 2,2-dimethyl-L-thiazolidine-4-carboxylic acid hydrochloride (277 mg, 1.4 mmol) and 2 equiv of DIPEA (0.49 mL, 2.8 mmol) in anhydrous DCM (20 mL). After 1 h reaction under argon atmosphere, the mixture was washed with 20 mL of aqueous solution of 10% (w/v) citric acid, dried, and concentrated in vacuo. The crude product was purified by silica gel column chromatography to give 425 mg of Fmoc-Gly-Cys-($\Psi^{Me,Me}$Pro)-OH (69% yield). ^{1}H NMR (250 MHz, $CDCl_3$): δ 7.76−7.73 (m, 2H), 7.59−7.56 (m, 2H), 7.42−7.26 (m, 4H), 5.76 (br, 1H), 4.77−4.75 (m, 1H), 4.36−4.17 (m, 3H), 4.03−3.94 (m, 2H), 3.38−3.29 (m, 2H), 1.89 (s, 3H), 1.84 (s, 3H). ESI-MS: m/z calculated for $C_{23}H_{24}N_2O_5S$ 440.14, found 463.13 [M + Na$^+$].

Cys($\Psi^{Me,Me}$Pro)-containing peptides were similarly synthesized on Rink Resin LS, which had been modified with a 4-hydroxymethylbenzoic acid linker. Coupling of the first residue was carried out with 5 equiv of *N*,*N*′-diisopropylcarbodiimide, 5 equiv of Fmoc-amino acid, and 5 equiv of hydroxybenzotriazole for 3 h. Fmoc-Gly-Cys-($\Psi^{Me,Me}$Pro)-OH was incorporated by using 2 equiv of the dipeptide, 2 equiv of PyBOP, and 2 equiv of hydroxybenzotriazole. Fmoc-His(Mmt)-OH, Fmoc-Thr(Trt)-OH, and Fmoc-Glu(*O*-2-Phi*P*r)-OH

dx.doi.org/10.1021/jm500743t | J. Med. Chem. 2014, 57, 7792−7797

were incorporated using the standard Fmoc chemistry. After the peptide synthesis was complete, the resin was treated with 1% TFA and 5% triisopropylsilane in DCM for 2 h. The peptide was released from the resin with 1:1 (v/v) propylamine/DMF for 3 h.

To conjugate a peptide to R_{11}, the peptide containing an N-terminal amine (~10 μmol) was dissolved in 200 μL of 50 mM phosphate buffer (pH 8.0) and mixed with 1 equiv of SPDP dissolved in 100 μL of DMF. After incubation for 4 h at room temperature, 1 equiv of Ac-R_{11}-Cys-NH_2 was added to the mixture and incubated for 12 h (Figure S5 in SI). All peptides used in biochemical and cellular tests were purified by reversed-phase HPLC to ≥98% purity and the peptide identity was confirmed by MALDI-TOF MS analysis (Figure S2 in SI).

Fluorescence Anisotropy. Glutathione S-transferase−CN fusion protein was expressed in *Escherichia coli* BL21 cells and purified on a glutathione-Sepharose column as previously described.[31] FA experiments were performed by incubating 100 nM fluorescein-labeled peptide with varying concentrations of CN in 20 mM HEPES (pH 7.4), 150 mM NaCl, 2 mM $Mg(OAc)_2$, and 0.1% bovine serum albumin for 2 h at room temperature. The FA values were measured on a Molecular Devices Spectramax M5 spectrofluorimeter, with excitation and emission wavelengths at 485 and 525 nm, respectively. Dissociation constants (K_D) were determined by plotting the FA values as a function of the CN concentration and fitting the data to equation (Origin 9.0)

$$Y = \left\{A_{min} + (A_{max} \times Q_b/Q_f - A_{min}) \times \left[(L + x + K_D) - \sqrt{(L + x + K_D)^2 - 4 \times L \times x}\right]/2/L\right\} \Big/ \left\{1 + (Q_b/Q_f - 1) \times \left[(L + x + K_D) - \sqrt{(L + x + K_D)^2 - 4 \times L \times x}\right]/2/L\right\}$$

where Y is the FA value at a given concentration x of CN; L is the peptide concentration; Q_b/Q_f is the correction factor for fluorophore−protein interaction; A_{max} is the maximum FA value when all the peptide are bound to CN, while A_{min} is the minimum FA value when all of the peptides are free. The competition experiments were similarly carried out, except that each reaction contained fixed concentrations of FITC−ZIZIT (100 nM) and CN (150 nM) but varying concentrations of the competing peptide (0−20 μM).

■ ASSOCIATED CONTENT

Ⓢ Supporting Information

Additional experimental and molecular modeling details. This material is available free of charge via the Internet at http://pubs.acs.org.

■ AUTHOR INFORMATION

Corresponding Author

*Phone: (614) 688-4068. E-mail: pei.3@osu.edu.

Present Address

[§](T.L.) Department of Chemistry, The Scripps Research Institute, La Jolla, CA 92037.

Notes

The authors declare no competing financial interest.

■ ACKNOWLEDGMENTS

We thank Dr. Huiming Li for helpful discussions and Dr. Sara Cole for assistance with microscope imaging. Funding was from the National Institutes of Health (GM062820 and CA132855).

■ ABBREVIATIONS USED

CN, calcineurin; CsA, cyclosporine A; Tle, *tert*-leucine; FA, fluorescence anisotropy; NFAT, nuclear factor of activated T cells; PPI, protein−protein interaction

■ REFERENCES

(1) Crabtree, G. R. Generic signals and specific outcomes: signaling through Ca^{2+}, calcineurin, and NF-AT. *Cell* **1999**, *96*, 611−614.

(2) Rao, A.; Luo, C.; Hogan, P. G. Transcription factors of the NFAT family: regulation and function. *Annu. Rev. Immunol.* **1997**, *15*, 707−747.

(3) Liu, J.; Farmer, J. D.; Lane, W. S.; Friedman, J.; Weissman, I.; Schreiber, S. L. Calcineurin is a common target of cyclophilin−cyclosporine A and FKBP-FK506 complexes. *Cell* **1991**, *66*, 807−815.

(4) Kiani, A.; Rao, A.; Aramburu, J. Manipulating immune responses with immunosuppressive agents the target NFAT. *Immunity* **2000**, *12*, 359−372.

(5) Chapman, J. R. Chronic calcineurin inhibitor nephrotoxicity—lest we forget. *Am. J. Transplant.* **2011**, *11*, 693−697.

(6) Sigal, N. H.; Dumont, F.; Durette, P.; Siekierka, J. J.; Peterson, L.; Rich, D. H.; Dunlap, B. E.; Staruch, M. J.; Melino, M. R.; Koprak, S. L.; Williams, D.; Witzel, B.; Pisano, J. M. Is cyclophilin involved in the immunosuppressive and nephrotoxic mechanism of action of cyclosporine A? *J. Exp. Med.* **1991**, *173*, 619−628.

(7) Platz, K. P.; Mueller, A. R.; Blumhardt, G.; Bachmann, S.; Bechstein, W. O.; Kahl, A.; Neuhaus, P. Nephrotoxicity following orthotopic liver transplantation. A comparison between cyclosporine and FK506. *Transplantation* **1994**, *58*, 170−178.

(8) Hojo, M.; Morimoto, T.; Maluccio, M.; Asano, T.; Morimoto, K.; Lagman, K.; Shimbo, T.; Suthanthiran, M. Cyclosporine induces cancer progression by a cell-autonomous mechanism. *Nature* **1999**, *397*, 530−534.

(9) Aramburu, J.; Garcia-Cozar, F.; Raghavan, A.; Okamura, H.; Rao, A.; Hogan, P. G. Selective inhibition of NFAT activation by a peptide spanning the calcineurin targeting site of NFAT. *Mol. Cell* **1998**, *1*, 627−637.

(10) Li, H.; Rao, A.; Hogan, P. G. Interaction of calcineurin with substrates and targeting proteins. *Trends Cell Biol.* **2011**, *21*, 91−103.

(11) Roy, J.; Cyert, M. S. Cracking the phosphatase code: docking interactions determine substrate specificity. *Sci. Signalling* **2009**, *2*, re9.

(12) Grigoriu, S.; Bond, R.; Cossio, P.; Chen, J. A.; Ly, N.; Hummer, G.; Page, R.; Cyert, M. S.; Peti, W. The molecular mechanism of substrate engagement and immunosuppressant inhibition of calcineurin. *PLoS Biol.* **2013**, *11*, e1001492.

(13) Aramburu, J.; Yaffe, M. B.; Lopez-Rodriguez, C.; Cantley, L. C.; Hogan, P. G.; Rao, A. Affinity-driven peptide selection of an NFAT inhibitor more selective than cyclosporine A. *Science* **1999**, *285*, 2129−2133.

(14) Noguchi, H.; Matsushita, M.; Okitsu, T.; Moriwaki, A.; Tomizawa, K.; Kang, S.; Li, S. T.; Kobayashi, N.; Matsumoto, S.; Tanaka, K.; Tanaka, N.; Matsui, H. A new cell-permeable peptide allows successful allogeneic islet transplantation in mice. *Nature Med.* **2004**, *10*, 305−309.

(15) Sieber, M.; Baumgrass, R. Novel inhibitors of the calcineurin/NFATc hub—alternatives to CsA and FK506? *Cell Commun. Signaling* **2009**, *7*, 25.

(16) Li, H.; Zhang, L.; Rao, A.; Harrison, S. C.; Hogan, P. G. Structure of calcineurin in complex with PVIVIT peptide: portrait of a low-affinity signaling interaction. *J. Mol. Biol.* **2007**, *369*, 1296−1306.

(17) Takeuchi, K.; Roehrl, M. H.; Sun, Z. Y.; Wagner, G. Structure of the calcineurin−NFAT complex: defining a T cell activation switch using solution NMR and crystal coordinates. *Structure* **2007**, *15*, 587−597.

(18) Li, H.; Rao, A.; Hogan, P. G. Structural delineation of the calcineurin−NFAT interaction and its parallels to PP1 targeting interactions. *J. Mol. Biol.* **2004**, *342*, 1659−1674.

(19) Davies, S. J.; Ayscough, A. P.; Beckett, R. P.; Clements, J. M.; Doel, S.; Pratt, L. M.; Spavold, Z. M.; Thomas, S. W.; Whittaker, M.

Structure−activity relationships of the peptide deformylase inhibitor BB-3497: modification of the P2′ and P3′ side chains. *Bioorg. Med. Chem. Lett.* **2003**, *13*, 2715−2718.
(20) Llinas-Brunet, M.; Bailey, M. D.; Ghiro, E.; Gorys, V.; Halmos, T.; Poirier, M.; Rancourt, J.; Goudreau, N. A systematic approach to the optimization of substrate-based inhibitors of the hepatitis C virus NS3 protease: discovery of potent and specific tripeptide inhibitors. *J. Med. Chem.* **2004**, *47*, 6584−6594.
(21) Sigman, M. S.; Jacobsen, E. N. Schiff base catalysts for the asymmetric Strecker reaction identified and optimized from parallel synthetic libraries. *J. Am. Chem. Soc.* **1998**, *120*, 4901−4902.
(22) Bold, G.; Fassler, A.; Capraro, H.-G.; Cozens, R.; Klimkait, T.; Lazdins, J.; Mestan, J.; Poncioni, B.; Rusel, J.; Stover, D.; Tintelnot-Blomley, M.; Acemoglu, F.; Beck, W.; Boss, E.; Eschbach, M.; Hurlimann, T.; Masso, E.; Roussel, S.; Ucci-Stoll, K.; Wyss, D.; Lang, M. New aza-dipeptide analogues as potent and orally absorbed HIV-1 protease inhibitors: candidates for clinical development. *J. Med. Chem.* **1998**, *41*, 3387−3401.
(23) Perni, R. B.; Almquist, S. J.; Byrn, R. A.; Chandorkar, G.; Chaturvedi, P. R.; Coutney, L. F.; Decker, C. J.; Dinehart, K.; Gates, C. A.; Harbeson, S. L.; Heiser, A.; Kalkeri, G.; Kolaczkowski, E.; Lin, K.; Luong, Y.-P.; Rao, B. G.; Taylor, W. P.; Thomson, J. A.; Tung, R. D.; Wei, Y.; Kwong, A. D.; Lin, C. Preclinical profile of VX-950, a potent, selective, and orally bioavailable inhibitor of hepatitis C virus NS3-4A serine protease. *Antimicrob. Agents Chemother.* **2006**, *50*, 899−909.
(24) Wedemeyer, W. J.; Welker, E.; Scheraga, H. A. Proline *cis*−*trans* isomerization and protein folding. *Biochemistry* **2002**, *41*, 14637−14644.
(25) Dumy, P.; Keller, M.; Ryan, D. E.; Rohwedder, B.; Wohr, T.; Mutter, M. Pseudo-prolines as a molecular hinge: reversible induction of *cis* amide bonds into peptide backbones. *J. Am. Chem. Soc.* **1997**, *119*, 918−925.
(26) Chierici, S.; Jourdan, M.; Figuet, M.; Dumy, P. A case study of 2,2-dimethylthiazolidine as locked *cis* proline amide bond: synthesis, NMR and molecular modeling studies of a δ-conotoxin EVIA peptide analog. *Org. Biomol. Chem.* **2004**, *2*, 2436−2441.
(27) Wohr, T.; Wahl, F.; Nefzi, A.; Rohwedder, B.; Sato, T.; Sun, X.; Mutter, M. Pseudo-prolines as a solubilizing, structure-disrupting protection technique in peptide synthesis. *J. Am. Chem. Soc.* **1996**, *118*, 9218−9227.
(28) Luechapanichkul, R.; Chen, X.; Taha, H. A.; Vyas, S.; Guan, X.; Freitas, M. A.; Pei, D. Specificity profiling of dual specificity phosphatase vaccinia VH1-related (VHR) reveals two distinct substrate binding modes. *J. Biol. Chem.* **2013**, *288*, 6498−6510.
(29) Gwack, Y.; Sharma, S.; Nardone, J.; Tanasa, B.; Iuga, A.; Srikanth, S.; Okamura, H.; Bolton, D.; Feske, S.; Hogan, P. G.; Rao, A. A genome-wide Drosophila RNAi screen identifies DYRK-family kinases as regulators of NFAT. *Nature* **2006**, *441*, 646−650.
(30) Kaduk, C.; Wenschuh, H.; Beyermann, M.; Forner, K.; Carpino, L. A.; Bienert, M. Synthesis of Fmoc-amino acid fluorides via DAST, an alternative fluoridation agent. *Lett. Pept. Sci.* **1995**, *2*, 285−288.
(31) Kang, S.; Li, H.; Rao, A.; Hogan, P. G. Inhibition of the calcineurin−NFAT interaction by small organic molecules reflects binding at an allosteric site. *J. Biol. Chem.* **2005**, *280*, 37698−37706.